Analysis of separable potentials

Xavier Gonze*
Université Catholique de Louvain, Unité de Physico–Chimie et de Physique des Matériaux, 1, place Croix du Sud, B-1348, Louvain-La-Neuve, Brabant, Belgium

Roland Stumpf and Matthias Scheffler
Fritz-Haber-Institut der Max-Planck-Gesellschaft, Faradayweg 4-6, D-1000 Berlin 33, Federal Republic of Germany
(Received 24 April 1991)

Soft, fully separable *ab initio* pseudopotentials, introduced some years ago by Kleinman and Bylander [Phys. Rev. Lett. **48**, 1425 (1982)], have proven to be very useful for large-scale electronic-structure and total-energy calculations. However, these pseudopotentials can induce unphysical results and destroy important chemical properties of the atom in the solid, if not constructed cautiously. We present here a detailed analysis of Kleinman-Bylander separable pseudopotentials. Two different techniques (a spectral investigation, and the logarithmic-derivative construction) allow a deeper understanding of their properties. It is shown how the above-mentioned problems can be avoided.

I. INTRODUCTION

Electronic-structure calculations using pseudopotentials have recently seen a great increase in applications to many-atom systems, by the use of the Car-Parrinello molecular-dynamics technique.[1] One advantage of this method is that it avoids the need to diagonalize directly the Hamiltonian matrix. However, the evaluation of the Hamiltonian acting on a trial wave function is still a computationally expensive calculation when the usual form of nonlocal norm-conserving pseudopotentials[2] is used.

Soft, fully separable *ab initio* pseudopotentials, as proposed by Kleinman and Bylander[3] (KB pseudopotentials), achieve a substantial reduction of computing time needed to apply the Hamiltonian operator to wave functions. However, they can cause unphysical results if not constructed cautiously. While a warning was already given in the original KB paper, no rigorous understanding of the problems was available. Some authors[4] used KB separable potentials in studies of large-size systems that otherwise would have been intractable.

Recently, procedures[5,6] were designed to force the separability of the usual form of norm-conserving pseudopotentials,[2] but these were not as efficient as the use of the KB pseudopotentials. Moreover, it was realized[5,6] that some iterative diagonalization schemes[7] could efficiently use a separable form for nonlocal pseudopotentials. In order to avoid the difficulties, some empirical rules for generating reliable KB pseudopotentials were published by Bylander and Kleinman,[8] while Vanderbilt[9] and Blöch[10] proposed interesting generalizations of the KB form. Along the same line of thought, connections between linear augmented plane wave (LAPW) and pseudopotentials were exhibited.[11]

In a recent paper[12] Gonze, Käckell, and Scheffler published a brief description of a more fundamental investigation of KB pseudopotentials. Using selenium as an example, they showed the appearance of some rapid deviation of the logarithmic derivative from the all-electron one, resulting in a spurious bound state (ghost state). They also provided a theorem for the identification of such ghosts. Subsequently Stumpf, Gonze, and Scheffler compiled a list of fully separable *ab initio* pseudopotentials.[13]

In the present paper, the general theoretical framework for the analysis of KB pseudopotentials that was used in Refs. 12 and 13 is presented. Two different techniques (a spectral investigation and the logarithmic-derivative construction) allow a deeper understanding of their properties. Some applications will be presented.

In Sec. II, we recall the background notions: local, nonlocal, semilocal, and fully separable (KB) pseudopotentials. The fundamental differences between semilocal and fully separable pseudopotentials for the isolated atom are emphasized in Sec. III. For the former pseudopotentials, no ghost problems were reported. Indeed, we show that a corollary of the Wronskian theorem prevents the appearance of bound states below the reference atomic level. This theorem is not valid for fully separable pseudopotentials. We also propose an algorithm for the calculation of logarithmic derivatives.

Our discussion is complemented by a spectral analysis (Sec. IV), which leads to some absolute characterization of the KB pseudopotentials, in terms of a parametrized Hamiltonian. A "Kleinman-Bylander energy" (KB energy) explicitly characterizes the strength of the KB potential, while a "Kleinman-Bylander cosine" allows one to distinguish between an artificially or an intrinsically large KB energy.

In Sec. V, we present two theorems that are useful in the analysis of the KB Hamiltonian. A corollary of these two theorems has already been presented in Ref. 12: a criterion for the existence of a "ghost level" under the reference atomic energy level. We also show how to estimate the energy range for this ghost level.

The two complementary approaches (logarithmic derivative construction and spectral analysis) are then used to show how to correct a KB pseudopotential (Sec. VI). Simple and systematic ideas are developed. An in-

troduction to "A list of separable, norm-conserving pseudopotentials"[13] is then given and we use pseudopotentials from this list for the calculation of the GaAs band structure. Finally, we discuss briefly the application of the ideas in this paper to the pseudopotential forms introduced by Vanderbilt[9] and Blöch.[10] Atomic units (hartree) are used throughout, except when explicitly mentioned.

II. SEPARABLE PSEUDOPOTENTIALS

In the real-space representation, a nonlocal pseudopotential $\hat{V}$ is defined by a Hermitian kernel $V(\mathbf{r},\mathbf{r}')$, such that:

$$\langle \mathbf{r}|\hat{V}|\varphi\rangle = \int V(\mathbf{r},\mathbf{r}')\varphi(\mathbf{r}')d\mathbf{r}' \ . \tag{1}$$

The atom is centered at the origin. Introducing spherical symmetry, the kernel only depends on $\rho=|\mathbf{r}|$, $\rho'=|\mathbf{r}'|$, and the cosine between $\mathbf{r}$ and $\mathbf{r}'$. Expanding the kernel in Legendre polynomials with respect to this cosine, and using the addition theorem for spherical harmonics, we obtain the following general expression for energy-independent Hermitian pseudopotentials, in spherical coordinates $\mathbf{r}(\theta,\phi,\rho),\mathbf{r}'(\theta',\phi',\rho')$:

$$V(\mathbf{r},\mathbf{r}')=\sum_{l,m} Y^*_{l,m}(\theta,\phi)V_l(\rho,\rho')Y_{l,m}(\theta',\phi') \ . \tag{2}$$

In this equation, there is one and only one Hermitian kernel $V_l(\rho,\rho')$ for each angular momentum l, and this kernel is a function of the one-dimensional radial variables ρ and ρ' only.

In the common form of nonlocal pseudopotentials,[2-17] the kernel is diagonal:

$$V_l(\rho,\rho')=V_l(\rho)\delta(\rho-\rho') \ . \tag{3}$$

Such a form is called *semilocal* (radially local, but angularly nonlocal). By contrast, a *local* potential, which is also characterized by a dirac function $\delta(\rho-\rho')$, does not depend on the angular momentum l. It acts locally also in the angular coordinates.

Outside the cutoff radius, an ionic pseudopotential (semilocal or general) has to reduce to the all-electron ionic potential (which is local). Taking advantage of the increasing centrifugal barrier for large l, a nonlocal potential can be expressed as the sum of a local part and some short-ranged nonlocal corrections for only a few angular momenta ($l\le l_{\max}$). Thus we get, for a general nonlocal potential

$$V_l(\rho,\rho')=V^{\rm loc}(\rho)\delta(\rho-\rho')+\Delta V_l(\rho,\rho') \quad \text{for } l\le l_{\max} \ , \tag{4}$$

for a semilocal potential, we obtain

$$V_l(\rho,\rho')=V^{\rm loc}(\rho)\delta(\rho-\rho')+\Delta V_l^{\rm SL}(\rho)\delta(\rho-\rho') \quad \text{for } l\le l_{\max} \ , \tag{5}$$

and, in both cases,

$$V_l(\rho,\rho')=V^{\rm loc}(\rho)\delta(\rho-\rho') \quad \text{for } l> l_{\max} \ . \tag{6}$$

Note that inside the cutoff radius, the local potential $V^{\rm loc}$ will be nearly arbitrary, as soon as the nonlocal corrections $\Delta V_l(\rho,\rho')$ are designed so as to reproduce the correct kernels V_l for each angular momentum $l\le l_{\max}$.

In order to guarantee sufficient transferability, Hamann, Schlüter, and Chiang[2] (HSC) defined the norm-conserving condition and generated semilocal norm-conserving pseudopotentials (see also Ref. 15). Bachelet, Hamann, and Schlüter (BHS) applied the HSC scheme to generate a table of pseudopotentials for 94 elements. This table is often used in common practice.

For fully separable pseudopotentials, *the ρ and ρ' dependences of the nonlocal potential are disconnected:*

$$\Delta V_l(\rho,\rho')=F_l^*(\rho)f_lF_l(\rho') \ . \tag{7}$$

Mixing the angular and radial dependences [Eqs. (2) and (7)] into single three-dimensional functions, we have

$$\Delta V(\mathbf{r},\mathbf{r}')=\sum_{l,m}\xi^*_{l,m}(\mathbf{r})f_l\xi_{l,m}(\mathbf{r}') \tag{8}$$

or, using the dirac bra-ket notation, this reads

$$\Delta\hat{V}=\sum_{l,m}|\xi_{l,m}\rangle f_l\langle\xi_{l,m}| \ . \tag{9}$$

Thus a separable potential is a sum of projectors.

Notice that a given $\Delta\hat{V}$ operator can be cast into this form in different ways. Indeed, there is one degree of freedom in the choice of the wave vectors and coefficient, given by

$$\Delta\hat{V}=\sum_{l,m}|\alpha_l\xi_{l,m}\rangle\frac{f_l}{|\alpha_l|^2}\langle\alpha_l\xi_{l,m}| \ , \tag{10}$$

where α_l is an arbitrary number.

Kleinman and Bylander[3] gave a construction formula for the generation of *norm-conserving* separable pseudopotentials. They connected the separable nonlocal parts to the semilocal parts defined in the HSC scheme,[2] or in the BHS table[14]:

$$\Delta\hat{V}^{\rm KB}=\sum_{l,m}\frac{|\Delta V_l^{\rm SL}\phi^{\rm ps}_{l,m}\rangle\langle\phi^{\rm ps}_{l,m}\Delta V_l^{\rm SL}|}{\langle\phi^{\rm ps}_{l,m}|\Delta V_l^{\rm SL}|\phi^{\rm ps}_{l,m}\rangle} \ , \tag{11}$$

where $\phi^{\rm ps}_{l,m}$ is the HSC reference pseudo-wave-function of angular momentum l [$\phi^{\rm ps}_{lm}(\mathbf{r})=Y_{l,m}(\theta,\phi)R_l^{\rm ps}(\rho)$] and $\Delta V_l^{\rm SL}$ is the HSC (Ref. 2) semilocal correction to the local potential [see also Eq. (5)]. The constant f_l in the general expression Eq. (9) corresponds to the inverse of the matrix elements in the denominator of Eq. (11).

The KB formula connecting the fully separable form to the semilocal form is unique in the following sense: if we (a) require that

$$\Delta\hat{V}^{\rm KB}|\phi^{\rm ps}_{l,m}\rangle=|\Delta V_l^{\rm SL}\phi^{\rm ps}_{l,m}\rangle \ , \tag{12}$$

and (b) use the form of Eq. (7), then we recover Eq. (11), with a unique degree of freedom described by the factor α in Eq. (10).

If we rely on other semilocal pseudopotential generating schemes,[16,17] the result will be similar to Eq. (11). The presence of the denominator in Eq. (11) can induce some problems in the scattering properties of the potential as well as ghost states, as we will see in detail in Secs. III and IV.

III. PROBLEMS WITH FULLY SEPARABLE PSEUDOPOTENTIALS

In Ref. 12 we described problems induced by the use of the KB pseudopotential constructed from the BHS table, with the help of Eq. (11), using selenium as an example. A ghost state appears at 80 eV below the vacuum level, well below the zero-node reference wave function. The logarithmic derivative also differs strongly from the all-electron logarithmic derivative.

For semilocal potentials the problems encountered with fully separable pseudopotentials do not occur. The following simple argument gives the essential reason for the difference between semilocal and fully separable potentials.

Let us consider each angular momentum separately, and construct the radial differential equation governing the behavior of the radial wave function. We use the following notations: three-dimensional partial wave at energy ε,

$$\phi_{l,m}(\mathbf{r},\varepsilon)=Y_{l,m}(\theta,\phi)R_l(\rho,\varepsilon) \tag{13}$$

and one-dimensional radial function at energy ε,

$$u_l(\rho,\varepsilon)=R_l(\rho,\varepsilon)\rho \ . \tag{14}$$

For a semilocal potential, the equation for the function $u_l(\rho,\varepsilon)$, at energy ε, is

$$-\frac{1}{2}\frac{d^2u_l}{d\rho^2}+\bar{V}_l^{\rm loc}(\rho)u_l(\rho,\varepsilon) +\Delta V_l^{\rm SL}(\rho)u_l(\rho,\varepsilon)-\varepsilon u_l(\rho,\varepsilon)=0 \ , \tag{15}$$

while for a general nonlocal potential (including KB), it is

$$-\frac{1}{2}\frac{d^2u_l}{d\rho^2}+\bar{V}_l^{\rm loc}(\rho)u_l(\rho,\varepsilon) +\int \Delta V_l(\rho,\rho')u_l(\rho',\varepsilon)d\rho'-\varepsilon u_l(\rho,\varepsilon)=0 \ . \tag{16}$$

$\bar{V}_l^{\rm loc}$ contains the local part of the pseudopotential as well as the centrifugal potential (angular momentum dependent), and the hartree and the exchange-correlation potential if the problem is treated self-consistently. At any energy ε, Eq. (15) is an *ordinary* differential equation, where we recognize the kinetic-energy operator (second-order derivative), the local potential contribution, and the semilocal one, which has exactly the same form as the local one. By contrast, Eq. (16) is an *integrodifferential* equation, because the nonlocal part of the pseudopotential does not reduce to a simple multiplication.

Without any further investigation, there is an important difference between the semilocal and fully separable pseudopotentials. Indeed, for an ordinary differential equation, we have the following corollary of the Wronskian theorem:[18] "If one arranges the eigenstates in the order of increasing energies $\varepsilon_0,\varepsilon_1,\ldots,\varepsilon_n$, the eigenfunctions likewise fall in the order of increasing number of nodes." As it was pointed out in Ref. 12, this corollary does *not* hold for the integrodifferential equation (16).

As a consequence it is possible that bound states appear at lower energies than the *zero-node* reference atomic level. These unphysical states were termed "ghost states" in Ref. 12. They should have at least one node, because due to the Hermiticity of the Hamiltonian they have to be orthogonal to the zero-node atomic reference wave function, and two zero-node functions cannot be orthogonal to each other. The same argument does not rule out the possibility that *two one-node functions* were solutions of Eq. (16). As a consequence, the classification, as well as the characterization of wave functions with respect to the number of nodes, have to be abandoned.

The calculation of logarithmic derivatives, an important tool for the analysis of differential equations, is not obvious for fully separable potentials. Taking Eqs. (7) and (16) we obtain

$$-\frac{1}{2}\frac{d^2u_l}{d\rho^2}+\bar{V}_l^{\rm loc}(\rho)u_l(\rho,\varepsilon) +F_l^*(\rho)f_l\int F_l(\rho')u_l(\rho',\varepsilon)d\rho'-\varepsilon u_l(\rho,\varepsilon)=0 \ . \tag{17}$$

The usual algorithms (e.g., Runge-Kutta and predictor-corrector) to solve ordinary differential equations, and construct logarithmic derivatives, are inadequate owing to the integral part in Eq. (17). We took a computationally efficient, stable, and simple method similar to the Fredholm method for integral equations.[9] The basic idea is to consider the value of the integral in Eq. (17) first as a constant factor, and solve the resulting inhomogeneous ordinary differential equation. In a second step, a closure formula will reintroduce the dependence of the integral on the wave function. Explicitly, the algorithm reads as follows.

(i) Find the general solution of the homogeneous equation and a special solution of the inhomogeneous equation without any integral part:

$$-\frac{1}{2}\frac{d^2W}{d\rho^2}+\bar{V}_l^{\rm loc}(\rho)W(\rho,\varepsilon)-\varepsilon W(\rho,\varepsilon)=0 \tag{18}$$

and

$$-\frac{1}{2}\frac{d^2X}{d\rho^2}+\bar{V}_l^{\rm loc}(\rho)X(\rho,\varepsilon)-\varepsilon X(\rho,\varepsilon)=F_l^*(\rho) \ . \tag{19}$$

These equations can be solved for any energy using predictor-corrector algorithms, for example.

(ii) Construct the integrals

$$\tilde{W}(\varepsilon)=f_l\int F_l(\rho)W(\rho,\varepsilon)d\rho \tag{20}$$

and

$$\tilde{X}(\varepsilon)=1+f_l\int F_l(\rho)X(\rho,\varepsilon)d\rho \ . \tag{21}$$

(iii) The solution of the integrodifferential equation is then given by

$$u(\rho,\varepsilon)=K[W(\rho,\varepsilon)\tilde{X}(\varepsilon)-X(\rho,\varepsilon)\tilde{W}(\varepsilon)] \ , \tag{22}$$

where K is a normalization factor.

Our procedure[20] is different from the one proposed by Bylander and Kleinman,[8] and does not need any iterative solution for a given energy.

IV. SPECTRAL ANALYSIS

Following the line of thought of Sec. III, we consider each angular momentum l separately. As the angular behavior is factored out, only one-dimensional quantities will be handled. We first explain the basic notations for this one-dimensional analysis. The Hamiltonian that enters the radial Schrödinger equation (16) can be split into three parts: the kinetic-energy operator, the local potential (including the centrifugal barrier), and the nonlocal correction. In the case of a fully separable part, we have

$$\hat{H}_l^{\mathrm{KB}}=\hat{T}+\hat{\tilde{V}}_l^{\mathrm{loc}}+\frac{|\Delta V_l^{\mathrm{SL}}u_l^{\mathrm{ps}}\rangle\langle u_l^{\mathrm{ps}}\Delta V_l^{\mathrm{SL}}|}{\langle u_l^{\mathrm{ps}}|\Delta V_l^{\mathrm{SL}}|u_l^{\mathrm{ps}}\rangle} . \tag{23}$$

Here, the meaning of the bra-ket notation is

$$\langle u_l^{\mathrm{ps}}|\Delta V_l^{\mathrm{SL}}|u_l^{\mathrm{ps}}\rangle=\int_0^{\infty}u_l^{\mathrm{ps}}(\rho)^*\Delta V_l^{\mathrm{SL}}(\rho)u_l^{\mathrm{ps}}(\rho)d\rho . \tag{24}$$

The u_l^{ps} are the reference eigenfunctions of the semilocal Hamiltonian[21] (as well as the KB Hamiltonian), with eigenvalue E_l^{ps}. We introduce also the corresponding local Hamiltonian, defined by Eq. (23) but leaving away the nonlocal part:

$$\hat{H}_l^{\mathrm{loc}}=\hat{T}+\hat{\tilde{V}}_l^{\mathrm{loc}} . \tag{25}$$

The eigenvalues of the local Hamiltonian are labeled $E_{l,0}E_{l,1},E_{l,2},\ldots$ The eigenvalues of the local Hamiltonian are consistently ordered with respect to the number of nodes of the wave functions (the spectrum is "well behaved").

The spectral analysis aims to characterize the nonlocal part of the KB Hamiltonian, and to understand the modifications brought by this nonlocal part to the well-behaved local Hamiltonian spectrum. To achieve this, we define the KB operator for angular momentum l:

$$\Delta\hat{V}_l^{\mathrm{KB}}=\frac{|\Delta V_l^{\mathrm{SL}}u_l^{\mathrm{ps}}\rangle\langle u_l^{\mathrm{ps}}\Delta V_l^{\mathrm{SL}}|}{\langle u_l^{\mathrm{ps}}|\Delta V_l^{\mathrm{SL}}|u_l^{\mathrm{ps}}\rangle} , \tag{26}$$

which is added to the local Hamiltonian to generate the KB Hamiltonian.

We now consider the following eigenvector of the KB operator: $|\Delta V_l^{\mathrm{SL}}u_l^{\mathrm{ps}}\rangle$. It satisfies the eigenvalue equation

$$\Delta\hat{V}_l^{\mathrm{KB}}|\Delta V_l^{\mathrm{SL}}u_l^{\mathrm{ps}}\rangle=E_l^{\mathrm{KB}}|\Delta V_l^{\mathrm{SL}}u_l^{\mathrm{ps}}\rangle , \tag{27}$$

with the eigenvalue given by

$$E_l^{\mathrm{KB}}=\frac{\langle u_l^{\mathrm{ps}}\Delta V_l^{\mathrm{SL}}|\Delta V_l^{\mathrm{SL}}u_l^{\mathrm{ps}}\rangle}{\langle u_l^{\mathrm{ps}}|\Delta V_l^{\mathrm{SL}}|u_l^{\mathrm{ps}}\rangle} . \tag{28}$$

This eigenvalue will be called Kleinman-Bylander energy (KB energy). We introduce also the normalized eigenvector

$$|u_l^{\mathrm{KB}}\rangle=\frac{|\Delta V_l^{\mathrm{SL}}u_l^{\mathrm{ps}}\rangle}{(\langle u_l^{\mathrm{ps}}\Delta V_l^{\mathrm{SL}}|\Delta V_l^{\mathrm{SL}}u_l^{\mathrm{ps}}\rangle)^{1/2}} . \tag{29}$$

Using these definitions, the KB operator reduces to the following projector:

$$\Delta\hat{V}_l^{\mathrm{KB}}=|u_l^{\mathrm{KB}}\rangle E_l^{\mathrm{KB}}\langle u_l^{\mathrm{KB}}| . \tag{30}$$

Equation (30) provides a canonical form of Eq. (9). Indeed, as mentioned in Sec. II, the functions F_l and factors f_l are not unique: differently scaled F_l and f_l could give the same nonlocal operator [compare Eq. (10)]. By contrast, E_l^{KB} is uniquely defined.

Owing to the fact that $|u_l^{\mathrm{KB}}\rangle$ is normalized, E_l^{KB} is an *energy characterization* of the separable part of the pseudopotential. The KB energy gives the order of magnitude of the energy modifications brought to the local Hamiltonian spectrum where the KB operator is added to it. It should be obvious that if E_l^{KB} is large, the modification of the well-behaved local Hamiltonian spectrum will be large as well. We will analyze these modifications in Sec. V.

Examination of Eq. (28) shows that the KB energy can sometimes be quite large. ΔV_l^{SL} appears twice in the numerator, and only once in the denominator. If ΔV_l^{SL} is large, the KB energy will be "intrinsically" large. On the other hand, if the denominator nearly vanishes, the KB energy will also be large: the evaluation of the matrix element

$$\langle u_l^{\mathrm{ps}}|\Delta V_l^{\mathrm{SL}}|u_l^{\mathrm{ps}}\rangle=\int_0^{\infty}u_l^{\mathrm{ps}}(\rho)^*\Delta V_l^{\mathrm{SL}}(\rho)u_l^{\mathrm{ps}}(\rho)d\rho \tag{31}$$

involves the integral of the square of the norm of the wave function, which is always positive, multiplied by the quantity $\Delta V_l^{\mathrm{SL}}(\rho)$, which can be somewhere positive and somewhere negative. Weighted by $|u_l^{\mathrm{ps}}(\rho)|^2$, the negative and positive parts of $\Delta V_l^{\mathrm{SL}}(\rho)$ can nearly compensate, leading to an accidentally small denominator, and an "artificially large" KB energy.

We would like to measure quantitatively the extent to which a KB energy is intrinsically or artificially large. Note that u_l^{ps} is a normed function. We define the root-mean-square value $\Delta V_l^{\mathrm{rms}}$ of the potential $\Delta V_l^{\mathrm{SL}}(\rho)$ as

$$(\Delta V_l^{\mathrm{rms}})^2=\langle(\Delta V_l^{\mathrm{SL}})^2\rangle=\langle u_l^{\mathrm{ps}}|(\Delta V_l^{\mathrm{SL}})^2|u_l^{\mathrm{ps}}\rangle . \tag{32}$$

This quantity appears in the *numerator* of the KB energy, and characterizes the intrinsic strength of the potential. The ratio between $\Delta V_l^{\mathrm{rms}}$ and the KB energy E_l^{KB} (the latter combines intrinsic as well as artificial influences) is

$$C_l^{\mathrm{KB}}=\frac{\Delta V_l^{\mathrm{rms}}}{E_l^{\mathrm{KB}}}=\frac{\langle u_l^{\mathrm{ps}}|\Delta V_l^{\mathrm{SL}}|u_l^{\mathrm{ps}}\rangle}{(\langle u_l^{\mathrm{ps}}\Delta V_l^{\mathrm{SL}}|\Delta V_l^{\mathrm{SL}}u_l^{\mathrm{ps}}\rangle)^{1/2}}$$
$$=\langle u_l^{\mathrm{KB}}|u_l^{\mathrm{ps}}\rangle . \tag{33}$$

C_l^{KB} is also equal to the cosine between $|u_l^{\mathrm{ps}}\rangle$ and $|\Delta V_l^{\mathrm{SL}}u_l^{\mathrm{ps}}\rangle$. As a cosine,

$$-1<C_l^{\mathrm{KB}}<1 . \tag{34}$$

The inverse of this KB cosine gives the artificial factor of enhancement of the energy scale $\Delta V_l^{\mathrm{rms}}$ which leads to the KB energy E_l^{KB}:

$$E_l^{\mathrm{KB}}=\frac{1}{C_l^{\mathrm{KB}}}\Delta V_l^{\mathrm{rms}} . \tag{35}$$

It is now evident that if the KB cosine is nearly zero, E_l^{KB} will be large.

To illustrate these points, we give in Table I numerical values for the pseudopotentials of eight elements. We use pseudopotentials of Ref. 14 with the d potential as local, and define the s and p nonlocal corrections with respect to this local potential.

The KB energies run from -381 to 6624 eV, and have their smallest absolute value as -2 eV. The KB cosine values range from -0.60 to 0.33, with the smallest absolute value as 0.002 02. From our experience (see Sec. VII), we will use the C^{KB} absolute value of 0.15 as the limit between artificially and intrinsically large KB energy. Seven KB energy absolute values (from the total of 16 in Table I) are quite large (absolute value above 100 eV). Having a look at the corresponding KB cosine, we see that the KB energies for carbon p and oxygen s and p are mainly intrinsic, while they are mainly artificial in the other four cases. The As s state is especially dramatic: the KB energy is 6624 eV. The corresponding KB cosine, which is equal to 0.002 02, leads to an enhancement factor of 495 with respect to the characteristic energy ΔV_s^{rms}.

The KB energy and cosine are indicators that we will use to correct the KB pseudopotentials (see Sec. VI).

TABLE I. KB energies E^{KB} and KB cosine C^{KB} for pseudopotentials of eight elements. s and p angular momenta are considered. The pseudopotentials are taken for the BHS (Ref. 14) table, with the d potential used as a local potential.

		E^{KB} (eV)	C^{KB}
C	s	84	0.33
	p	-189	-0.18
O	s	168	0.33
	p	-381	-0.18
Al	s	63	0.31
	p	32	0.26
Si	s	93	0.31
	p	51	0.27
Ga	s	-62	-0.13
	p	-2	-0.60
Ge	s	-190	-0.055
	p	-4	-0.41
As	s	6624	0.0020
	p	-17	-0.16
Se	s	332	0.050
	p	-190	-0.022

V. THE PARAMETRIZED HAMILTONIAN

For a further analysis of the modification to the local Hamiltonian brought by the KB operator we introduce the following *parametrized* Hamiltonian:

$$\hat{H}^{KB}(\lambda)=\hat{H}^{loc}+|u^{KB}\rangle\lambda\langle u^{KB}| , \tag{36}$$

where $\hat{H}^{loc}$ and the KB wave function *are fixed* (note that any reference to angular momentum indices l has been suppressed in this section), while the quantity λ is considered a parameter that can take any value between $-\infty$ and $+\infty$. Of course, if the parameter λ vanishes, we recover the local Hamiltonian, while if $\lambda=E^{KB}$, we recover the true KB Hamiltonian.

The spectrum $E_0(\lambda)$, $E_1(\lambda)$, ... of this parametrized Hamiltonian can be considered as a function of the parameter λ. The indices of the eigenvalues correspond to the energy ordering of the levels, and are in general not a node classification.

In order to find out the evolution of each eigenenergy curve as a function of λ we consider first a finite-dimensional space of dimension N. $\hat{H}^{KB}(\lambda)$ has exactly N real eigenvalues and N orthogonal eigenvectors, because the studied Hamiltonian is Hermitian (mathematically, the Hamiltonian is equivalent to a Hermitian matrix).

Theorem 1. Each eigenenergy curve $E_i(\lambda)$ is an increasing function of λ with

$$0\leq\frac{dE_i(\lambda)}{d\lambda}\leq 1 . \tag{37}$$

The proofs of this theorem and the following one are given in the Appendix.

Theorem 2. At the asymptotic limit of very large absolute values of λ the parametrized Hamiltonian can be split into three terms:

$$\hat{H}^{KB}(\lambda)=P\hat{H}^{loc}P+|\tilde{u}^{KB}\rangle\tilde{\lambda}\langle\tilde{u}^{KB}|+O\left[\frac{1}{\lambda}\right] . \tag{38}$$

The last term is asymptotically small. The first term acts in a dimension $(N-1)$-space, and is independent of λ. It is the projection of the local Hamiltonian on some subspace, by the projector operator $P=1-|u^{KB}\rangle\langle u^{KB}|$ (which is independent of λ). The second term acts in a one-dimensional space, which is orthogonal to the previously mentioned $(N-1)$-dimensional space, in the large λ asymptotic limit. $\tilde{\lambda}$ and $\tilde{u}^{KB}$ are defined as

$$\tilde{\lambda}=\lambda+\langle u^{KB}|\hat{H}^{loc}|u^{KB}\rangle \tag{39}$$

and

$$|\tilde{u}^{KB}\rangle=|u^{KB}\rangle+\frac{1}{\lambda}P\hat{H}^{loc}|u^{KB}\rangle . \tag{40}$$

Note that $\tilde{\lambda}$ is a linear function of λ, with slope 1, and that the wave function $\tilde{u}^{KB}$ reduces to u^{KB} in the asymptotic limit.

The two theorems impose strong requirements on the shape of the spectrum. A typical example is shown in Fig. 1. Note the monotonic increase of each eigenenergy

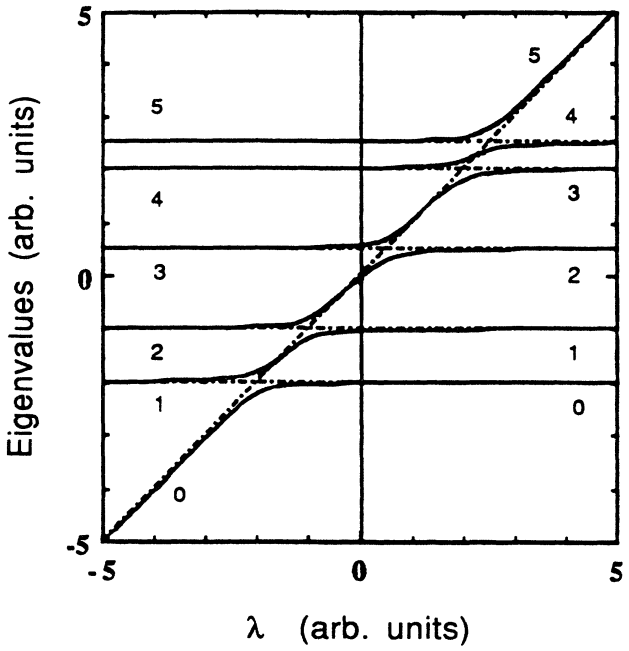

FIG. 1. Solid lines: the eigenvalues $E_i(\lambda)$ of a typical parametrized Hamiltonian $\hat{H}^{\mathrm{KB}}(\lambda)$ [Eq. (36)], numbered from 0 to 5, according to their energy. The dimension of the vector space is 6. Dash-dotted lines are straight lines having the same asymptotic behavior as the eigenvalues. The difference between the two sets of lines is mainly the avoided crossings of eigenvalues.

curve (from theorem 1), as well as the asymptotic behavior: one linear component and $N-1$ constant components. In the medium-energy range, we find avoided crossings between different levels, which are due to the third term of Eq. (38), as well as to the difference between $\tilde{u}^{\mathrm{KB}}$ and u^{KB}.

To analyze this graph, let us introduce a negative energy λ^- and a positive energy λ^+. The first theorem imposes that

$$E_i(-\infty)<E_i(\lambda^-)<E_i(0)<E_i(\lambda^+)<E_i(+\infty)\ . \tag{41}$$

The second theorem connects the values at $-\infty$ and at $+\infty$. Indeed, all the asymptotic values of energies corresponding to the constant term (first term) of Eq. (38) are identical in the $-\infty$ and $+\infty$ cases, except that their numbering is different. This can be seen in Fig. 1. The first level at $-\infty$ is the linearly increasing one (numbered 0 in Fig. 1), while the linear level at large values of λ is the highest in energy (numbered 5). So, the energy of the second level at $-\infty$ (numbered 1) is the energy of the first level at $+\infty$ (numbered 0), the energy of the third level at $-\infty$ (numbered 2) is the energy of the second level at $+\infty$ (numbered 1), and so on. To summarize,

$$E_{i+1}(-\infty)=E_i(+\infty)\ . \tag{42}$$

Using these results we obtain the following connection between the spectrum of the nonlocal KB Hamiltonian, and the corresponding local Hamiltonian (for which $\lambda=0$): for a positive energy λ^+,

$$E_0(0)<E_0(\lambda^+)<E_1(0)<E_1(\lambda^+)<E_2(0)<\cdots\ ; \tag{43}$$

for a negative energy λ^-,

$$E_0(\lambda^-)<E_0(0)<E_1(\lambda^-)<E_1(0)<E_2(\lambda^-)<\cdots\ . \tag{44}$$

These results are true for any λ [Eq. (43) if λ is positive, Eq. (44) if λ is negative], thus they also hold for the "true" KB energy, i.e., $\lambda=E^{\mathrm{KB}}$. The structure of Eqs. (43) and (44) is quite simple: we get successively one eigenenergy of the local Hamiltonian and one eigenenergy of the KB Hamiltonian. The difference between Eqs. (43) and (44) lies only in the way in which the series begins: the ground state of the *local* Hamiltonian if λ is positive, or the ground state of the KB Hamiltonian if λ is negative. This difference will be important for the correction procedure in Sec. VI.

The corresponding analysis of a parametrized Hamiltonian in an *infinite-dimension space*, but with a short-range KB operator $\Delta\hat{V}$ is given in the Appendix. It shows that below the continuum, the conclusions of the finite-dimension space analysis are still valid [Eqs. (41)–(44)]. Up to the continuum, we can rely on the classification of the KB Hamiltonian eigenenergies with respect to the local Hamiltonian eigenenergies, Eqs. (43) and (44). As a corollary of this classification, we have the following criterion[12] for the existence of a bound state *under* the reference atomic level (a ghost state), for any angular momentum l.

(i) $E_l^{\mathrm{KB}}>0$. There is a ghost level under the atomic reference level if, and only if, the atomic reference eigenvalue is higher in energy than the first excited level of the local Hamiltonian.

(ii) $E_l^{\mathrm{KB}}<0$. There is a ghost level under the atomic reference level if, and only if, the atomic reference eigenvalue is higher in energy than the ground-state of the local Hamiltonian.

Indeed, in the first case, due to the classification explained below, Eq. (43), we are sure that the KB Hamiltonian will also give a level between the ground state and the first excited state of the local Hamiltonian. This level will be below the atomic reference level (note that the eigenvalues of the local Hamiltonian are given in Fig. 1 on the $\lambda=0$ axis). Q.E.D.

For the second case the proof is analogous.

Table II gives some examples of the application of this criterion. Again, we have taken the potentials from the BHS table, using the d potential as local, for the eight elements in Table I. From the application of the criterion, we are sure of the existence of a ghost in the case of selenium p angular momentum and also in the case of germanium s angular momentum [case (ii) of our criterion]. In the other cases, we have no ghost under the atomic reference level. The first ghost (in selenium) was identified in Ref. 12, at -80 eV. We also checked that a

self-consistent calculation, performed using a plane-wave basis set, considering the atom in a very large box, produced this same ghost level. In the self-consistent procedure, this ghost level was of course not occupied. The large *positive* KB energy observed in As does not produce a ghost level, but generates instabilities when used in Car-Parrinello[1] simulations.[22] For gallium, a ghost exists, but is found above the atomic reference level. It is easily identified in logarithmic derivative plots. As we will see in Sec. VI, it induces a modification of the conduction bands in GaAs, but the valence bands and their density are only weakly affected.

Could we get an indication of the energy of the germanium ghost without resorting to the calculation in a large box, or to the radial Schrödinger equation solution? It is easy to get a lower bound for the ground state of the parametrized Hamiltonian. Indeed, this ground state is equal to the following expectation value:

$$E_0(\lambda)=\langle u_0(\lambda)|\hat{H}^{\mathrm{KB}}(\lambda)|u_0(\lambda)\rangle\ , \tag{45}$$

$$E_0(\lambda)=\langle u_0(\lambda)|\hat{H}^{\mathrm{loc}}|u_0(\lambda)\rangle + \langle u_0(\lambda)|u^{\mathrm{KB}}\rangle\lambda\langle u^{\mathrm{KB}}|u_0(\lambda)\rangle\ , \tag{46}$$

where $|u_0(\lambda)\rangle$ is the ground-state wave function of the parametrized Hamiltonian. This ground-state energy is certainly higher in energy than the sum of the lowest possible value of each term of Eq. (46), which give the following estimates for $\lambda=E^{\mathrm{KB}}$:

$$E_0(E^{\mathrm{KB}})>E_0(0)+E^{\mathrm{KB}} \tag{47}$$

if the KB energy is negative, and

$$E_0(E^{\mathrm{KB}})>E_0(0) \tag{48}$$

if the KB energy is positive.

We can also get an upper bound for the ground state of the parametrized Hamiltonian using the fact that the slope of the ground-state curve is lower than +1 [from Eq. (39)]. Its asymptotic behavior is given by Eq. (39), which has a slope exactly equal to +1 (see the dash-dotted curve of slope +1 in Fig. 1). Thus this linear function of λ is always greater than the ground-state energy curve (the ground-state energy curve is the lowest solid curve of Fig. 1). When $\lambda=E^{\mathrm{KB}}$ is large and negative, E^{KB} should closely approximate the energy of the ghost state $E^0(E^{\mathrm{KB}})$ as seen in Fig. 1.

If the $\lambda=E^{\mathrm{KB}}$ is negative, the ground state of the local Hamiltonian provides another upper bound (due to Theorem 1). If the KB energy is positive, the energy of the first excited state of the local Hamiltonian provides one upper bound, Eq. (43). In this case, another upper bound is also provided by the following quantity:

$$E_0(0)+E^{\mathrm{KB}}\ , \tag{49}$$

obtained using Theorem I applied to the ground-state curve starting at zero KB energy.

From this, we get the following estimation of the germanium ghost energy: between −90.5 and −202.9 eV. From the radial Schrödinger equation resolution, we can get the numerical value of −114 eV.

We may also mention that this type of Hamiltonian defined in Eq. (36) and analyzed above has been recently studied in a different context. In particular, their soliton-like behavior has received some interest (see, for example, Ref. 23).

TABLE II. Local Hamiltonian ground-state and first excited-state eigenvalues, atomic reference eigenvalues, and signs of KB energy for the pseudopotentials of eight elements. Pseudopotentials are taken from the BHS table (Ref. 14), with the *d* potential used as a local potential.

		E_0 (eV)	E_1 (eV)	E^{ps} (eV)	sign E^{KB}
C	*s*	−35.2	−1.1	−13.6	+
	p	−3.0	0.0	−5.4	−
O	*s*	−70.0	−1.4	−23.8	+
	p	−4.2	0.0	−9.2	−
Al	*s*	−35.8	−2.6	−7.8	+
	p	−10.5	−0.2	−2.8	+
Si	*s*	−55.4	−4.0	−10.9	+
	p	−17.9	−0.3	−4.2	+
Ga	*s*	−8.9	−0.5	−9.1	−
	p	−2.2	0.0	−2.7	−
Ge	*s*	−12.9	−0.7	−11.9	−
	p	−3.4	0.0	−4.0	−
As	*s*	−17.2	−0.8	−14.7	+
	p	−5.0	0.0	−5.3	−
Se	*s*	−22.0	−1.0	−17.4	+
	p	−6.73	0.0	−6.65	−

VI. APPLICATIONS

A. Logarithmic derivatives and ghost states

From the analysis performed in Secs. IV and V, it follows that an artificially large, negative KB energy is likely to generate a ghost level well below the reference atomic eigenlevel. This is why KB pseudopotentials sometimes fail for *s*- and *p*-bonded elements (when the *d* pseudopotential is chosen as the local potential). In this case, we will propose a very systematic way to avoid ghost states as well as erroneous logarithmic derivatives. If the KB energy is not artificially large negative, the idea developed in this section will still be useful, while less efficient.

The construction procedure described by Hamann, Schlüter, and Chiang[2] has its practical extensive realization in the BHS table.[14] In order to avoid the mentioned problems with fully separable potentials it is sometimes

necessary to use other starting semilocal potentials. Still following the technique of Hamann, Schlüter, and Chiang for generating the pseudopotentials, at least two kinds of parameters could be chosen different from the ones adopted by Bachelet, Hamann, and Schlüter:[14] the parameters defining the cutoff radii r_c for each angular momentum [see Eq. (5) of Ref. 12], and the exponent defining the shape of the pseudo-wave-functions [Eq. (2.12) of Ref. 14]. While the latter parameter is found to have little effect, varying the cutoff radii greatly changes the KB characteristics. Therefore we take the following approach: without significantly modifying the local Hamiltonian and the KB wave function [Eq. (36)], we try to make the denominator of the KB energy successively vanish and become positive. In the case of an artificially large KB energy, a slight modification of the cutoff radius will usually change the sign of the small denominator, while leaving the other parts of the parametrized Hamiltonian unchanged. By this transformation, the KB energy becomes first infinitely negative, then infinitely positive, then decreases quite fast to a reasonable positive value.

The effect of such a modification can be understood by reference to Fig. 1. Indeed, the spectrum of the parametrized Hamiltonian, while slightly modified due to the change in $H^{\rm loc}$ and $u^{\rm KB}$, will keep the general behavior represented in this figure. From the KB energy passing through infinity, from negative to positive, we see that the lower-lying level is sent to a large positive energy. Thus we succeed in removing an existing ghost level. The change of the KB energy from negative to positive corresponds also to the change of the criterion to be applied for the recognition of the existence of a ghost level. The deviation of the logarithmic derivative from the all-electron one is usually associated with such a ghost level. Thus removal of the ghost level simultaneously corrects the logarithmic derivative. An example of our procedure can be found in Ref. 12, where the BHS pseudopotential for selenium has been analyzed and modified.[24]

Bylander and Kleinman[8] recently suggested three rules that should also allow one to correct KB pseudopotentials. From our treatment (Secs. IV and V), we can analyze their proposal.

Their first rule [the $\Delta V_l(r)$ should be made as small and as short ranged as possible] corresponds to avoiding intrinsically large KB energies.

Their second rule [when the semilocal potentials $V_l(r)$ are significantly dissimilar—so that $\Delta V_l(r)$ cannot be small—the positive $\Delta V_l(r)$ should be made small], could work in the case of *intrinsically* large KB energies, as a criterion to choose the local potential. However, in the case of s- and p-bonded elements, the only problems we found arose from *artificially* large $E^{\rm KB}$. As a consequence, we find that this rule is in general not a good concept for creating pseudopotentials for these elements. We have seen that our correction procedure increases the positive part of ΔV. By contrast, in the case of transition metals, the large KB energy of these elements is intrinsic, thus difficult to modify. The d potential is too deep, compared to the s or p potentials. Therefore a change of the local potential seems to be the best solution.

Their third rule (the ratio $\langle u|\Delta V|u\rangle/\langle u\|\Delta V\|u\rangle$ should be as close to unity as possible and in no case less than 0.5) uses a notion similar to our KB cosine construction [see Eq. (33)]. Nevertheless, we have shown that negative KB cosines are often adequate, and that small absolute values for KB cosines (below 0.15) are dangerous only if they induce large KB energies, due to Eq. (35).

B. A list of separable pseudopotentials

The procedure described above has been used to construct fully separable potentials for 30 elements in the Periodic Table. We have compiled all the results, numerical as well as graphical, in Ref. 13 and now describe briefly the content of this report.

For each of the elements treated, we have provided (1) an analytical fit of the s, p, and d pseudopotentials, in the same form as in the BHS table; (2) an alternative to (1): the tabulated numerical values of pseudopotentials *and*

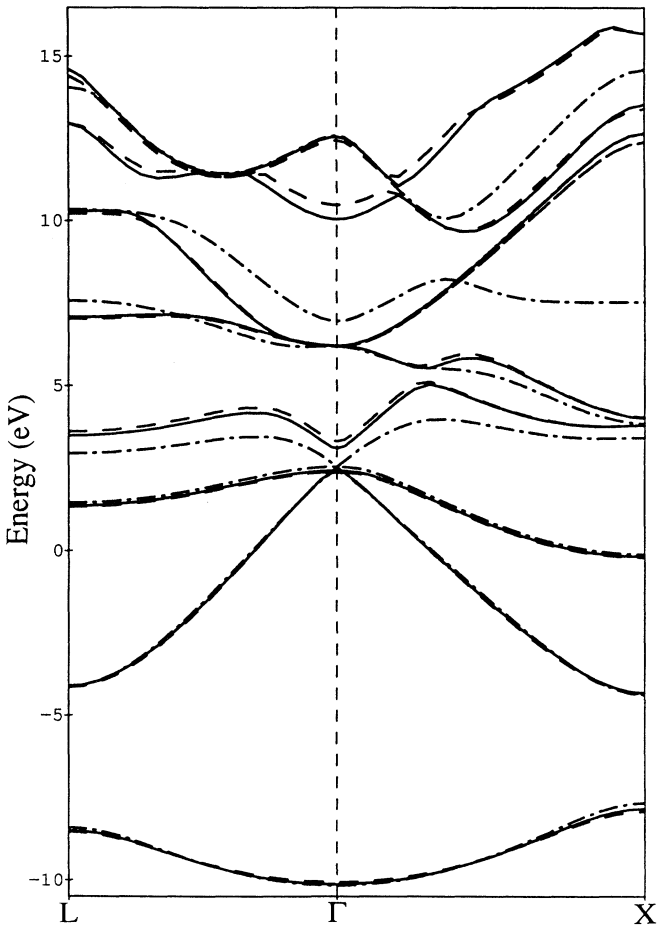

FIG. 2. GaAs band structure. Solid curve: result using the semilocal pseudopotential from the BHS table (Ref. 14). Dash-dotted curve: result using the separable pseudopotential based on the BHS table (Ref. 14). Dashed curve: result using the separable pseudopotential based on our table (Ref. 13). The $l=2$ potential has been used as a local potential.

wave functions, in order to be able to generate directly the KB form [Eq. (11)]; (3) the graphical presentation of the pseudopotential; and (4) plots of logarithmic derivatives, and comparison with the corresponding all-electron and semilocal results.

As an example we discuss now briefly the gallium-arsenide band structure. We have done a density-functional-theory[25] calculation with the Ceperley-Alder exchange-correlation potential as parametrized by Perdew and Zunger,[26] in the framework of the momentum-space formalism.[27] The cutoff for the kinetic energy of plane waves was fixed at 7.5 hartree, and the number of special points[28] for the integration in the irreducible Brillouin zone was equal to 2. From the BHS table,[14] using the semilocal form with the d potential as local, we get the band structure represented by solid curves in Fig. 2. Using the corresponding separable pseudopotential [Eq. (11)], we obtain the dash-dotted curves of Fig. 2. While the valence bands look good, we find strong modifications of the gap (decrease from 1.2 to 0.4 eV), as well as of the conduction bands, due to an atomic ghost state (here slightly above the reference atomic state) which strongly hybridizes in the region of 0.3–8.0 eV above the top of the valence band. These strong modifications can be related to the large deviation of the galllium separable pseudopotential (BHS based) s logarithmic derivative curve with respect to the semilocal s logarithmic derivative curve, as shown in Fig. 3. If we now use our pseudopotentials of Ref. 13, we find the band structure represented by dashed lines in Fig. 2, without any conduction ghost band, and a reasonable overall agreement with semilocal BHS result. The difference of about 0.2 eV at the gap can be traced to a slight difference between s logarithmic curves as shown in Fig. 3.

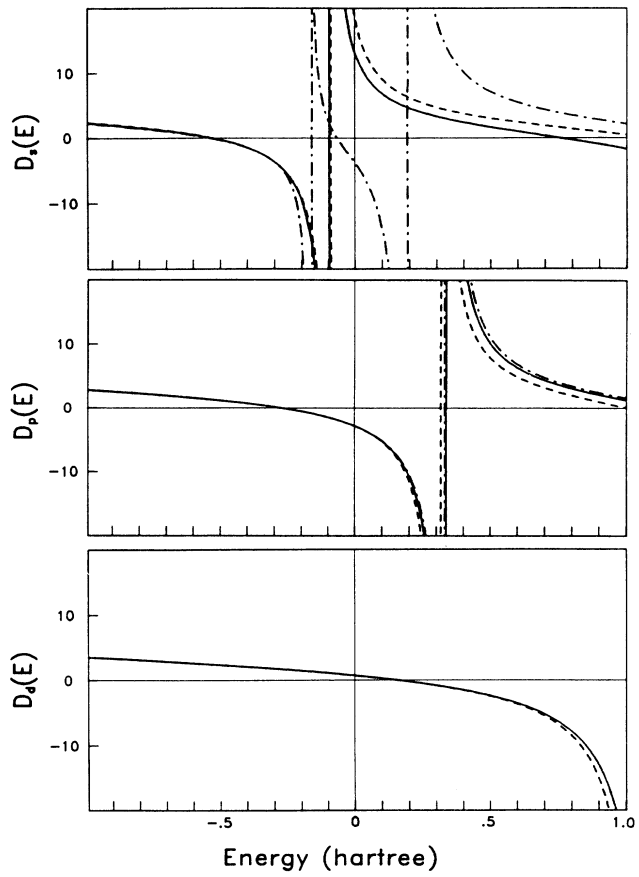

FIG. 3. Logarithmic derivatives for the s (top), p (middle), and d (bottom) states of the Ga atom. Solid curve: results using the semilocal pseudopotential from BHS table (Ref. 14). Dash-dotted curve: results using the separable pseudopotential based on BHS table (Ref. 14). Dashed curve: results using the separable pseudopotential based on our table (Ref. 13). The $l=2$ potential has been used as local potential.

C. Generalizations

As mentioned in the Introduction, Vanderbilt[9] and Blöchl[10] have proposed very interesting generalizations of the KB construction. The concepts developed in the present paper can be used to analyze these proposals. Although one of their aims is to avoid the spurious behavior found for fully separable pseudopotentials, it is worth mentioning that for these potentials the corollary of the Wronskian theorem still does not hold, and that the tools presented here are useful in understanding the properties of these potentials. In particular, the logarithmic derivative construction Eqs. (18)–(22) generalizes easily.

VII. CONCLUSION

In the present paper, we present an analysis of fully separable pseudopotentials. At first, we define the notion and indicate the problems that could arise when using fully separable potentials in quantum-mechanical calculations. In particular, we discuss the possible existence of extra bound levels (ghost levels) under the reference atomic eigenenergy which are allowed for fully separable pseudopotentials, but not for usual semilocal energy-independent pseudopotentials. An algorithm for logarithmic derivative construction, which had already been applied in Ref. 12, is also described. Logarithmic derivatives provide useful information on KB pseudopotentials, but should be complemented by a spectral analysis that also makes apparent the mathematical structure of KB pseudopotentials. With this spectral analysis the KB Hamiltonian can be written in a parametrized form. Using this form, we demonstrate two important theorems that lead to a deeper understanding of the KB Hamiltonian properties. The use of these tools enables one to correct the KB pseudopotentials generated using the HSC scheme. We use them to suppress the ghost level of selenium and to generate a table of separable pseudopotentials with application to the GaAs band structure. Finally, we discuss briefly some generalizations of KB pseudopotentials.

ACKNOWLEDGMENTS

We thank P. Käckell for his help in the beginning of this work, and D. C. Allan for critical reading of the

manuscript. One of us (X.G.) acknowledges the hospitality of the Fritz-Haber-Institut der Max-Plack-Gesellshaft (Berlin), as well as financial support from the National Fund for Scientific Research (Belgium).

APPENDIX

In this appendix, we analyze the parametrized Hamiltonian

$$\hat{H}^{\mathrm{KB}}(\lambda)=\hat{H}^{\mathrm{loc}}+|u^{\mathrm{KB}}\rangle\lambda\langle u^{\mathrm{KB}}| \ . \tag{A1}$$

As a first step, we consider the Hamiltonian $\hat{H}^{\mathrm{KB}}(\lambda)$ in a *finite-dimensional space of dimension N* (mathematically, the Hamiltonian is equivalent to a matrix). We assume that $\hat{H}^{\mathrm{loc}}$ is Hermitian (no other information on $\hat{H}^{\mathrm{loc}}$ is assumed in this first part of this appendix), that λ is real, and that u^{KB} is normalized. We will prove the two theorems mentioned in Sec. V.

By construction, $H^{\mathrm{KB}}(\lambda)$ is Hermitian. It has exactly N orthonormal eigenvectors $u_i(\lambda)$, which form a complete set of vectors. The corresponding N real eigenvalues are written $E_i(\lambda)$. The label i runs from 0 to $N-1$, and is ordered with respect to increasing eigenvalues. It is important to note that the set of eigenvectors as well as their eigenenergies will differ for each value of λ.

Theorem 1. Each eigenenergy curve $E_i(\lambda)$ is an increasing function of λ.

Proof:

$$\frac{dE_i(\lambda)}{d\lambda}=\frac{d}{d\lambda}[\langle u_i(\lambda)|\hat{H}^{\mathrm{KB}}(\lambda)|u_i(\lambda)\rangle] \ . \tag{A2}$$

Because $u_i(\lambda)$ are normalized and the parametrized Hamiltonian is Hermitian we obtain

$$\frac{dE_i(\lambda)}{d\lambda}=\left\langle u_i(\lambda)\left|\frac{d\hat{H}^{\mathrm{KB}}(\lambda)}{d\lambda}\right|u_i(\lambda)\right\rangle \ , \tag{A3}$$

$$\frac{dE_i(\lambda)}{d\lambda}=\langle u_i(\lambda)|u^{\mathrm{KB}}\rangle\langle u^{\mathrm{KB}}|u_i(\lambda)\rangle \ , \tag{A4}$$

$$\frac{dE_i(\lambda)}{d\lambda}=|\langle u_i(\lambda)|u^{\mathrm{KB}}\rangle|^2>0 \ . \tag{A5}$$

Q.E.D.

We also have the following subsidiary results: the quantity in Eq. (A5) is the square of a cosine because $u_i(\lambda)$ and u^{KB} are normalized. Thus it is lower than 1, which provides an upper bound for the slope of each eigenenergy curve. Because the set of eigenfunctions $u_i(\lambda)$ is a complete set we also obtain

$$\sum_i|\langle u_i(\lambda)|u^{\mathrm{KB}}\rangle|^2=1 \tag{A6}$$

and

$$\sum_i\frac{dE_i(\lambda)}{d\lambda}=1 \ . \tag{A7}$$

Theorem 2. The asymptotic behavior of the parametrized Hamiltonian (A1) is described by the following equation:

$$\hat{H}^{\mathrm{KB}}(\lambda)=P\hat{H}^{\mathrm{loc}}P+|\tilde{u}^{\mathrm{KB}}\rangle\tilde{\lambda}\langle\tilde{u}^{\mathrm{KB}}|+O\left[\frac{1}{\lambda}\right] \ . \tag{A8}$$

The last term vanishes in the case of large λ. The first term is independent of λ. The second one has a linear dependence, given by

$$\tilde{\lambda}=\lambda+\langle u^{\mathrm{KB}}|\hat{H}^{\mathrm{loc}}|u^{\mathrm{KB}}\rangle \ . \tag{A9}$$

The definition of $|\tilde{u}^{\mathrm{KB}}\rangle$ is

$$|\tilde{u}^{\mathrm{KB}}\rangle=|u^{\mathrm{KB}}\rangle+\frac{1}{\lambda}P\hat{H}^{\mathrm{loc}}|u^{\mathrm{KB}}\rangle \ . \tag{A10}$$

The projector P is equal to

$$P=1-|u^{\mathrm{KB}}\rangle\langle u^{\mathrm{KB}}| \ , \tag{A11}$$

and, in the asymptotic limit, the first term of Eq. (A8) acts in an $(N-1)$-dimensional space orthogonal to the one-dimensional space in which the second term acts.

Proof. The parametrized Hamiltonian is given by Eq. (A1). When λ is large (either positive or negative), we can consider the first term as a perturbation to the second term. This is certainly appropriate, if we deal with a finite vector space. We obtain directly one eigenvalue and one eigenfunction:

$$E(\lambda)=\lambda+\langle u^{\mathrm{KB}}|\hat{H}^{\mathrm{loc}}|u^{\mathrm{KB}}\rangle+O\left[\frac{1}{\lambda}\right] \tag{A12}$$

and

$$|u(\lambda)\rangle=|u^{\mathrm{KB}}\rangle+\frac{1}{\lambda}P\hat{H}^{\mathrm{loc}}|u^{\mathrm{KB}}\rangle+O\left[\frac{1}{\lambda^2}\right] \ . \tag{A13}$$

We now express the Hamiltonian, in terms of the quantities defined by Eqs. (A9) and (A10), that comes from Eqs. (A12) and (A13) truncated after order 1 and $1/\lambda$, respectively. This gives Eq. (A8). Q.E.D.

We now consider the *infinite-dimension case,* investigating the form encountered in practice: the pseudopotential is the sum of a separable nonlocal part, which is *short ranged,* and a *local* part, which can be short or long ranged, depending on the charge state of the system and on the treatment of exchange and correlation. The asymptotic value of the potential at infinite distance is taken as zero.

From Sec. III, one may see that the logarithmic derivative found at r_c is a single-valued function of the energy, always decreasing, except at poles (this property is implied by the norm-conserving condition). This behavior is found for any value of the KB energy. The important fact is that this behavior is qualitatively identical to the behavior of the logarithmic derivative found when a local potential is used. This means that the ranges of energy in which the spectrum is either discrete or continuous are not determined by the short-range sum of local and nonlocal pseudopotentials, but by the local potential that is found *outside* the cutoff radius. The continuum edge is thus independent of the short-ranged nonlocal potential and appears when the energy is larger than zero. Below

this energy, we find a discrete spectrum.

We now consider the two theorems demonstrated previously. It is immediate that Theorem 1 is valid in the discrete spectrum, while in the continuum spectrum, the consideration of one particular level is meaningless. The conclusions of the second theorem are also valid in the discrete spectrum: there is one asymptotically linear level, while all the other levels are asymptotically constant. The results of the infinite-dimensional space analysis are simple: the physical picture of the finite-dimensional analysis is preserved in the discrete spectrum range of energies.

Of course, in the solid-state applications, one introduces periodic conditions and finite basis sets. This restores a finite-dimensional space, for which the analysis has already been done.

---

*Present address: Laboratory of Atomic and Solid State Physics, Clark Hall, Cornell University, Ithaca, NY 14853.

[1]R. Car and M. Parrinello, Phys. Rev. Lett. **55**, 2471 (1985).

[2]D. R. Hamann, M. Schlüter, and C. Chiang, Phys. Rev. Lett. **43**, 1494 (1979).

[3]L. Kleinman and D. M. Bylander, Phys. Rev. Lett. **48**, 1425 (1982).

[4]D. C. Allan and M. P. Teter, Phys. Rev. Lett. **59**, 1136 (1987); G. Galli, R. M. Martin, R. Car, and M. Parrinello, *ibid.* **62**, 555 (1989); **63**, 988 (1989); I. Stich, R. Car, and M. Parrinello, *ibid.* **63**, 2240 (1989).

[5]I. Stich, R. Car, M. Parrinello, and S. Baroni, Phys. Rev. B **39**, 4997 (1989).

[6]X. Gonze, J.-P. Vigneron and J.-P. Michenaud, J. Phys. Condens. Matter **1**, 525 (1989).

[7]See, for example, E. R. Davidson, J. Comput. Phys. **17**, 87 (1975); P. Bendt and A. Zunger, Solar Energy Research Institute Technical Report No. TP-212-1698, 1982 (unpublished); D. M. Wood and A. Zunger, J. Phys. A **18**, 1343 (1985).

[8]D. M. Bylander and L. Kleinman, Phys. Rev. B **41**, 907 (1990).

[9]D. H. Vanderbilt, Phys. Rev. B **41**, 7892 (1990).

[10]P. Blöchl, Phys. Rev. B **41**, 5415 1990).

[11]S. Goedeker and K. Maschke, Phys. Rev. B **42**, 8858 (1990); P. Blöchl (unpublished).

[12]X. Gonze, P. Käckell, and M. Scheffler, Phys. Rev. B **41**, 12 264 (1990).

[13]R. Stumpf, X. Gonze, and M. Scheffler, Fritz-Haber-Institut Research Report No. 1, April, 1990 (unpublished).

[14]G. B. Bachelet, D. R. Hamann, and M. Schlüter, Phys. Rev. B **26**, 4199 (1982).

[15]G. P. Kerker, J. Phys. C **13**, L189 (1980).

[16]D. H. Vanderbilt, Phys. Rev. B **32**, 8412 (1985).

[17]D. R. Hamann, Phys. Rev. B **40**, 2980 (1989).

[18]A. Messiah, *Quantum Mechanics, Volume 1* (North-Holland, Amsterdam, 1974), pp. 98–111.

[19]B. L. Moisewitsch, *Integral Equations* (Longman, London, 1977).

[20]Independently of us, D. Vanderbilt also used this algorithm to get the results of Ref. 9 (private communication).

[21]The reference wave functions u_l^{ps}, eigenstates of the one-dimensional local Hamiltonian, can be shown to be real. Nevertheless, for the sake of generality, we have written Eq. (24) as if they were complex, and have kept this option in the whole paper.

[22]Using the concepts developed in Ref. 12 and the present paper, the modification of the large KB energy to a more reasonable value (< 300 eV) is easy, in addition to restoring a good convergence rate for the Car-Parrinello algorithm.

[23]P. Gaspard, S. A. Rice, and K. Nakamura, Phys. Rev. Lett. **63**, 930 (1989).

[24]In Ref. 14, "cc_d" for Se is equal to 2.0. In order to explain the apparent discrepancy between the KB energies in Fig. 4 of Ref. 12 and the values quoted in Table I, the following facts should be pointed out. Bachelet, Hamann, and Schlüter (Ref. 14) state to determine r_{max} as the mean value of the spin-up and spin-down wave-functions maxima. We found, however, that they used the smaller value of both, i.e., the spin-up result. In order to construct Fig. 4 of Ref. 12, the procedure described in Ref. 12 was used, with a different r_{max} for spin-up and spin-down components. This is one difference between the results from Ref. 14 (used in Table I) and in Fig. 4 of Ref. 12. The other significant difference is that in Ref. 12 quadruple precision arithmetic was used in order to become numerically stable in the inversion of the Schrödinger equation.

[25]P. Hohenberg and W. Kohn, Phys. Rev. **136**, B864 (1964); W. Kohn and L. J. Sham, Phys. Rev. **140**, A1133 (1965).

[26]D. M. Ceperley and B. J. Alder, Phys. Rev. Lett. **45**, 566 (1980); J. P. Perdew and A. Zunger, Phys. Rev. B **23**, 5048 (1981).

[27]J. Ihm, A. Zunger, and M. L. Cohen, J. Phys. C **12**, 4409 (1979).

[28]H. J. Monkhorst and J. D. Pack, Phys. Rev. B **13**, 5188 (1976).